Glycobiology, 2021, vol. 31, no. 12, 1645–1654
https://doi.org/10.1093/glycob/cwab080
Advance Access Publication Date: 26 July 2021
Original Article

OXFORD

Microbial Biology

Revisiting N-glycosylation in *Halobacterium salinarum*: Characterizing a dolichol phosphate- and glycoprotein-bound tetrasaccharide

Zlata Vershinin[2], Marianna Zaretsky[2], Ziqiang Guan[3], and Jerry Eichler[1,2]

[2]Department of Life Sciences, Ben-Gurion University of the Negev, P.O. Box 653, Beersheva 84105, Israel, and
[3]Department of Biochemistry, Duke University Medical Center, 240 Nanaline Duke, Durham, NC 27710, USA

[1]To whom correspondence should be addressed: Tel: +972-8646-1343; Fax: +972-8647-9175; e-mail: jeichler@bgu.ac.il

Received 14 May 2021; Revised 15 June 2021; Accepted 19 July 2021

Abstract

Although *Halobacterium salinarum* provided the first example of N-glycosylation outside the Eukarya, much regarding such post-translational modification in this halophilic archaea remains either unclear or unknown. The composition of an *N*-linked glycan decorating both the S-layer glycoprotein and archaellins offers one such example. Originally described some 40 years ago, reports from that time on have presented conflicted findings regarding the composition of this glycan, as well as differences between the protein-bound glycan and that version of the glycan attached to the lipid upon which it is assembled. To clarify these points, liquid chromatography-electrospray ionization mass spectrometry was employed here to revisit the composition of this glycan both when attached to selected asparagine residues of target proteins and when bound to the lipid dolichol phosphate upon which the glycan is assembled. Such efforts revealed the *N*-linked glycan as corresponding to a tetrasaccharide comprising a hexose, a sulfated hexuronic acid, a hexuronic acid and a second sulfated hexuronic acid. When attached to dolichol phosphate but not to proteins, the same tetrasaccharide is methylated on the final sugar. Moreover, in the absence of the oligosaccharyltransferase AglB, there is an accumulation of the dolichol phosphate-linked methylated and disulfated tetrasaccharide. Knowing the composition of this glycan at both the lipid- and protein-bound stages, together with the availability of gene deletion approaches for manipulating *Hbt. salinarum*, will allow delineation of the N-glycosylation pathway in this organism.

Key words: Archaea, dolichol phosphate, glycoproteins, *Halobacterium salinarum*, N-glycosylation

Introduction

N-glycosylation, a post-translational modification in which glycans are assembled on lipid carriers and then transferred to selected Asn residues in target proteins, is performed by members of all three domains of life (Aebi 2013; Nothaft and Szymanski 2013; Jarrell et al. 2014). While the overall process shares similarities across evolution, various aspects of N-glycosylation are unique to Eukarya, Bacteria and Archaea. In the case of archaeal N-glycosylation, one finds degrees of diversity in terms of the lipid carrier upon which the *N*-linked glycan is assembled, the steps involved in *N*-linked glycan assembly and glycan composition and architecture not seen in the other two domains (Schwarz and Aebi 2011; Eichler 2013; Eichler and Guan 2017). Such diversity is exemplified by N-glycosylation in the haloarchaea *Halobacterium salinarum*, that species in which this post-translational modification was first reported outside the Eukarya (Mescher and Strominger 1976).

Based on biochemical studies conducted in the late 1980s, two different *N*-linked glycans decorating *Hbt. salinarum* glycoproteins

were described (Lechner and Wieland 1989). One of these, detected on both the surface (S)-layer glycoprotein, the sole component of the S-layer surrounding the cell (Lechner and Sumper 1987; Trachtenberg et al. 2000), and on archaellins, the building blocks of the archaellum, the archaeal swimming device (Jarrell and Albers 2012), was described as a linear tetrasaccharide comprising glucose (Glc) and three glucuronic acids (GlcA), with each GlcA being sulfated (Wieland et al. 1980, 1983, 1985). The sugar composition of the same glycan was also described as corresponding to a tetrasaccharide comprising Glc-$(GlcA)_2$-Glc or as the pentasaccharide Glc-$(GlcA)_3$-Glc (Wieland et al. 1985; Lechner et al. 1985a). Moreover, at least one GlcA unit was described as being replaced by iduronic acid (Wieland et al. 1986).

In addition to seeking to define the composition of this *N*-linked glycan, these earlier studies also provided initial insight into the biosynthesis of this moiety. Such efforts reported the *N*-linked glycan as being assembled on dolichol phosphate (DolP), rather than dolichol pyrophosphate, as employed in eukaryal N-glycosylation, or undecaprenol pyrophosphate, as recruited in bacterial N-glycosylation (Lechner et al. 1985b; Burda and Aebi 1999; Swiezewska and Danikiewicz 2005; Jones et al. 2009; Hartley and Imperiali 2012). Furthermore, sulfation of the tetrasaccharide GlcA units was deemed to occur at the DolP-bound stage (Lechner et al. 1985b). Finally, it was reported that the Glc found at the nonreducing end of DolP-bound tetrasaccharide Glc-$(GlcA)_2$-Glc or pentasaccharide Glc-$(GlcA)_3$-Glc was methylated, although no such methylation was observed in the protein-bound glycan (Lechner et al. 1985a). Inhibition of S-adenosylmethionine-dependent methylation prevented transfer of the DolP-bound glycan to target proteins, leading these authors to conclude that such transient methylation was necessary for transfer of the lipid-linked glycan to the protein. To date, this phenomenon has not been reported elsewhere.

Today, with a complete genome sequence for *Hbt. salinarum* available (Ng et al. 2000), as well as genetic tools for its manipulation (Peck et al. 2000), there is renewed interest in *Hbt. salinarum* N-glycosylation. Based on the ability of selected *Hbt. salinarum* genes to replace their counterparts known to participate in the assembly and attachment of an *N*-linked pentasaccharide in *Haloferax volcanii*, where N-glycosylation has been studied in detail (Jarrell et al. 2014), a putative *Hbt. salinarum* pathway used for biogenesis of the *N*-linked tetrasaccharide decorating the S-layer glycoprotein and archaellins was proposed (Kandiba and Eichler 2015). Subsequent efforts revealed that AglB, the archaeal oligosaccharyltransferase, delivers a DolP-linked tetrasaccharide comprising hexuronic acid (Hex)-hexuronic acid $(HexA)_3$ to selected Asn residues of *Hbt. salinarum* archaellins (Zaretsky et al. 2019). This study, however, failed to detect HexA sulfation.

Given the discrepancies of previous studies addressing the composition of the *N*-linked tetrasaccharide decorating *Hbt. salinarum* glycoproteins, as well as seemingly unique aspects of the N-glycosylation process in this haloarchaea, several of the conclusions drawn in these previous efforts were revisited, relying on experimental approaches not available at that time.

Results

In *Hbt. salinarum*, the S-layer glycoprotein is modified by a *N*-linked disulfated tetrasaccharide

Characterization of the glycan attached to 10 of 12 potential N-glycosylation sites of the *Hbt. salinarum* S-layer glycoprotein began with analysis of Asn-479 in the S-layer glycoprotein-derived peptide ^{475}SDAVNSSGGVKDNIDTSDFNQGVSSTSSIR^{504} by liquid chromatography-electrospray ionization mass spectrometry (LC-ESI MS) (Lechner and Sumper 1987; Wieland 1988). Following digestion of the S-layer glycoprotein with trypsin, the MS profile of the resulting fragments (Table SI) included a peak of *m/z* 1298.83, corresponding to $[M + 3H]^{3+}$ ion of the Asn-479-containing peptide modified by a tetrasaccharide comprising a hexose, a hexuronic acid and two sulfated hexuronic acids ($[M + 3H]^{3+}$ ion calculated *m/z* 1298.82; Figure 1A, left). The MS/MS profile of this peak revealed a breakdown pattern that included fragments of *m/z* 1272.37, 1245.54, 1213.63, 1186.81, 1155.02 and 1128.04, respectively consistent with the peptide modified with a hexose, two hexuronic acids and a sulfated hexuronic acid ($[M + 3H]^{3+}$ ion calculated *m/z* 1272.15), with a hexose and three hexuronic acids ($[M + 3H]^{3+}$ ion calculated *m/z* 1245.48), with a hexose, a hexuronic acid and a sulfated hexuronic acid ($[M + 3H]^{3+}$ ion calculated *m/z* 1213.48), with a hexose and two hexuronic acids ($[M + 3H]^{3+}$ ion calculated *m/z* 1186.81), with a hexose and a sulfated hexuronic acid ($[M + 3H]^{3+}$ ion calculated *m/z* 1154.81) and with a hexose and a hexuronic acid ($[M + 3H]^{3+}$ ion calculated *m/z* 1128.14; Figure 1A, right). These latter five peaks are more readily seen upon expansion of that region of the profile spanning *m/z* 1120–1250 (Figure 1A, right, inset).

When the same MS profile generated upon trypsinization of the S-layer glycoprotein was further examined, a peak of *m/z* 1272.18, consistent with the $[M + 3H]^{3+}$ ion of the Asn-479-containing peptide modified by a tetrasaccharide comprising a hexose, two hexuronic acids and a sulfated hexuronic acid (calculated *m/z* 1272.15), was detected (Figure 1B, left). The MS/MS profile of this peak revealed a breakdown pattern that included a major fragment of *m/z* 1245.68 (Figure 1B, right, upper panel) and more minor fragments of *m/z* 1213.67, 1186.97, 1154.24, 1128.35 and 1069.50, with these latter four peaks being more readily seen upon expansion of that region of the profile spanning *m/z* 1060–1220 (Figure 1B, right, inset). The major *m/z* 1245.68 breakdown product is consistent with the peptide modified with a hexose and three hexuronic acids, as described above ($[M + 3H]^{3+}$ ion calculated *m/z* 1245.48). The five more minor breakdown products identified in the MS/MS profile, respectively correspond to the peptide modified with a hexose, a hexuronic acid and a sulfated hexuronic acid ($[M + 3H]^{3+}$ ion calculated *m/z* 1213.48), with a hexose and two hexuronic acids ($[M + 3H]^{3+}$ ion calculated *m/z* 1186.81), with a hexose and a sulfated hexuronic acid ($[M + 3H]^{3+}$ ion calculated *m/z* 1154.81), with a hexose and a hexuronic acid ($[M + 3H]^{3+}$ ion calculated *m/z* 1128.14) and with a hexose ($[M + 3H]^{3+}$ ion calculated *m/z* 1069.47).

Finally, analysis of the same MS profile revealed the presence of a *m/z* 1245.52 species, corresponding to $[M + 3H]^{3+}$ ion of the Asn-479-containing peptide modified by a tetrasaccharide comprising a hexose and three hexuronic acids (calculated *m/z* 1245.48; Figure 1C, left). The MS/MS profile of this peak revealed a breakdown pattern that included fragments of *m/z* 1187.18, 1128.50, 1069.82 and 1015.76, respectively consistent with the peptide modified with a hexose and two hexuronic acids ($[M + 3H]^{3+}$ ion calculated *m/z* 1186.81), with a hexose and a hexuronic acid ($[M + 3H]^{3+}$ ion calculated *m/z* 1128.14), with a hexose ($[M + 3H]^{3+}$ ion calculated *m/z* 1069.47) and with no linked sugars ($[M + 3H]^{3+}$ ion calculated *m/z* 1015.47) (Figure 1C, right).

To determine whether additional glycosylated *Hbt. salinarum* S-layer glycoprotein Asn residues presented the same glycosylation profile, glycosylation of Asn-609 in the S-layer glycoprotein-derived peptide ^{607}VGNYTSGSPTGDQIR^{621}, generated upon digestion with

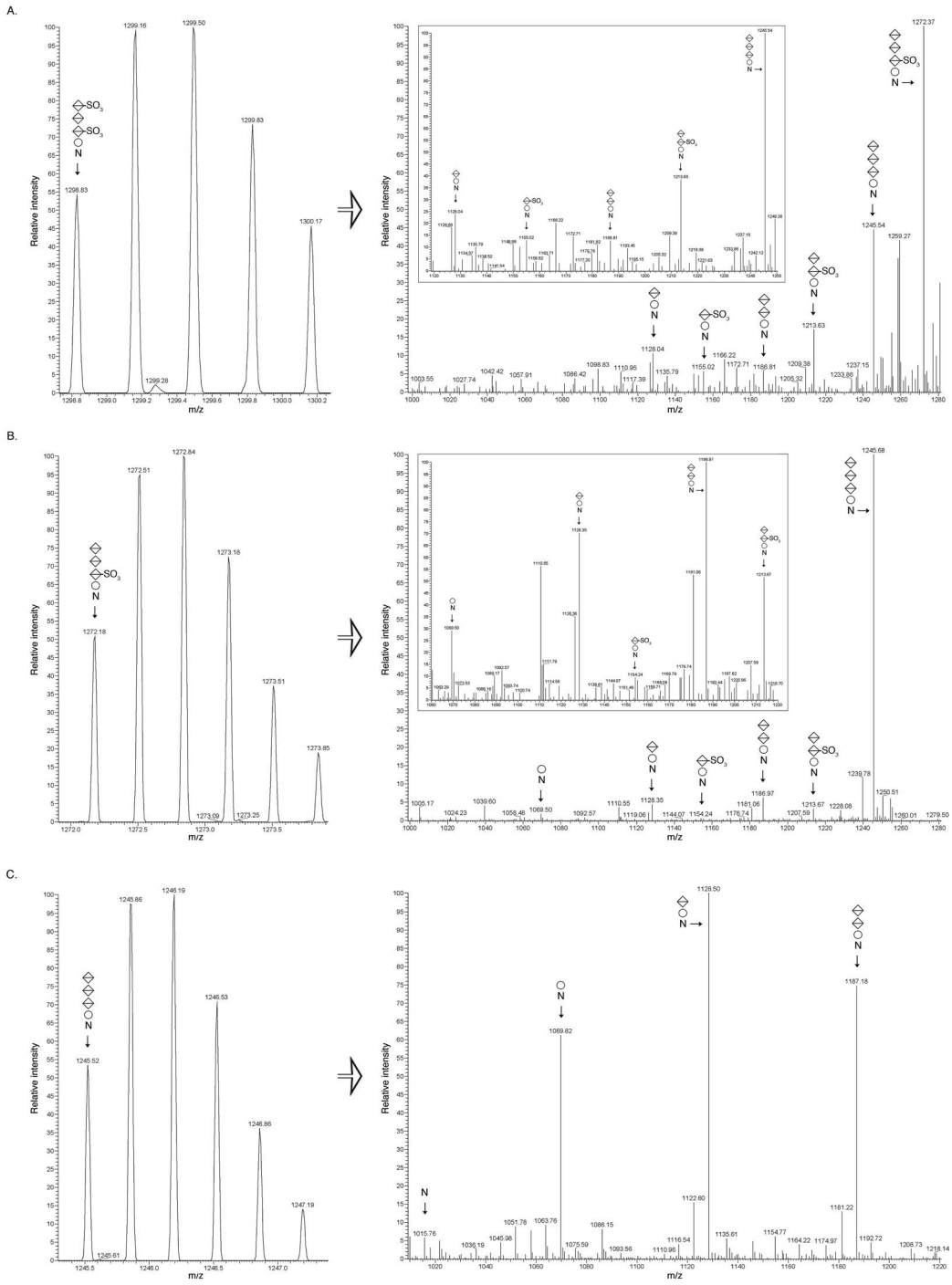

Fig. 1. *Halobacterium salinarum* S-layer glycoprotein Asn-479 is modified by a disulfated tetrasaccharide. LC-ESI MS (left panels) and MS/MS (right panels) identified an Asn-479-containing peptide modified by a tetrasaccharide comprising a hexose, a sulfated hexuronic acid, a hexuronic acid and a sulfated hexuronic acid (**A**), the same peptide modified by a tetrasaccharide comprising a hexose, two hexuronic acids and a sulfated hexuronic acid (**B**) and the same peptide modified by a tetrasaccharide comprising a hexose and three hexuronic acids (**C**). Selected regions of the MS/MS profiles are expanded to highlight specific peaks (right panels, insets). The circles correspond to hexoses, the split diamonds correspond to hexuronic acids and the N corresponds to the Asn-479-containing peptide.

trypsin and Glu-C protease, was assessed (Lechner and Sumper 1987). Here too, LC-ESI MS revealed the attachment of the same disulfated tetrasaccharide as described above (Figure S1).

The observed MS profiles and MS/MS breakdown patterns are thus consistent with the *Hbt. salinarum* S-layer glycoprotein being modified with a tetrasaccharide comprising a hexose as the linking

sugar, a sulfated hexuronic acid at position 2, a hexuronic acid at position 3 and a second sulfated hexuronic acid at position 4.

Hbt. salinarum archaellins are modified with the same *N*-linked glycan

Efforts were next directed as defining the N-glycosylation profile of FlaA1, FlaA2, FlaB1, FlaB2 and FlaB3, given how *Hbt. salinarum* archaellins were reported to be modified by the same *N*-linked tetrasaccharide as decorates the S-layer glycoprotein (Wieland et al. 1985). The MS profile of an *N*-glycosylated peptide common to FlaA2/FlaB1/FlaB3 (VDYV$^{56/80/56}$NLTVR, with the position of the modified asparagine in FlaA2, FlaB1 and FlaB3, respectively, indicated) generated upon digestion of these archaellins with trypsin and Glu-C protease offers a clear example of *Hbt. salinarum* archaellin N-glycosylation (Zaretsky et al. 2019) (Figure 2). The MS profile (Table SI) included a peak of *m/z* 964.83, corresponding to the $[M + 2H]^{2+}$ ion of the peptide modified by a tetrasaccharide comprising a hexose, a hexuronic acid and two sulfated hexuronic acids (calculated *m/z* 964.80) (Figure 2A, left). The MS/MS profile of this peak revealed a breakdown pattern that included fragments of *m/z* 924.66, 884.89, 836.69, 796.88, 748.48, 708.91 and 620.92, respectively consistent with the peptide modified with a hexose, a hexuronic acid and a sulfated hexuronic acid ($[M + 2H]^{2+}$ ion calculated *m/z* 924.80), with a hexose and three hexuronic acids ($[M + 2H]^{2+}$ ion calculated *m/z* 884.80), with a hexose, a hexuronic acid and a sulfated hexuronic acid ($[M + 2H]^{2+}$ ion calculated *m/z* 836.80), with a hexose and two hexuronic acids ($[M + 2H]^{2+}$ ion calculated *m/z* 796.80), with a hexose and a sulfated hexuronic acid ($[M + 2H]^{2+}$ ion calculated *m/z* 748.80), with a hexose and a hexuronic acid ($[M + 2H]^{2+}$ ion calculated *m/z* 708.80) and with a hexose ($[M + 2H]^{2+}$ ion calculated *m/z* 620.80) (Figure 2A, right). The latter five peaks are more readily seen upon expansion of that region of the profile spanning *m/z* 540–840 (Figure 2A, right, inset).

When the MS profile of the same peptide common to FlaA2, FlaB1 and FlaB3 was further examined, a peak of *m/z* 924.85, consistent with the $[M + 2H]^{2+}$ ion of the peptide modified by a tetrasaccharide comprising a hexose, two hexuronic acids and a sulfated hexuronic acid (calculated *m/z* 924.80), was seen (Figure 2B, left). The MS/MS profile of this peak revealed a breakdown pattern that included *m/z* 884.85, 836.39, 796.70 and 748.74 species (Figure 2B, right). These values correspond to the peptide modified with a hexose and three hexuronic acids, described above ($[M + 2H]^{2+}$ ion calculated *m/z* 884.80), with a hexose, a hexuronic acid and a sulfated hexuronic acid ($[M + 2H]^{2+}$ ion calculated *m/z* 836.80), with a hexose and two hexuronic acids ($[M + 2H]^{2+}$ ion calculated *m/z* 796.80) and with a hexose and a sulfated hexuronic acid ($[M + 2H]^{2+}$ ion calculated *m/z* 748.80). Expansion of that region of the MS/MS profile spanning *m/z* 540–840 highlighted the latter three of these species, as well as a *m/z* 620.88 peak, corresponding to the peptide modified with a hexose ($[M + 2H]^{2+}$ ion calculated *m/z* 620.80) (Figure 2B, right, inset).

Finally, the MS profile generated from FlaA2, FlaB1 and FlaB3 also included a *m/z* 884.87 species, consistent with the $[M + 2H]^{2+}$ ion of the peptide modified by a tetrasaccharide comprising a hexose and three hexuronic acids (calculated *m/z* 884.80) (Figure 2C, left). The MS/MS profile of this peak revealed a breakdown pattern that included *m/z* 796.87, 708.85, 620.85 and 539.85 species (Figure 2C, right). These values are consistent with the peptide modified with a hexose and two hexuronic acids ($[M + 2H]^{2+}$ ion calculated *m/z* 796.80), with a hexose and a hexuronic acid ($[M + 2H]^{2+}$ ion calculated *m/z* 708.80), with a hexose ($[M + 2H]^{2+}$ ion calculated *m/z* 620.80) and with the unmodified peptide ($[M + 2H]^{2+}$ ion calculated *m/z* 539.80).

Thus, as observed with two modified Asn residues of the *Hbt. salinarum* S-layer glycoprotein, Asn-56, Asn-80 and Asn-56, respectively found in FlaA2, FlaB1 and FlaB3 (as well as other Asn residues in this and other archaellins; Table SII), are also decorated with a tetrasaccharide comprising a hexose, a sulfated hexuronic acid, a hexuronic acid and a second sulfated hexuronic acid.

In an additional set of experiments, differential sulfation of the *Hbt. salinarum* archaellins (and the S-layer glycoprotein) in response to environmental conditions was considered. For this, *Hbt. salinarum* were grown in medium containing lower salt concentrations than the 4.2 M NaCl level normally found in the growth medium. Specifically, cells were grown in medium containing either 3.5 or 2.9 M NaCl. In each case, the archaellins (and the S-layer glycoprotein) presented the same MS profiles as when the cells were grown in the presence of 4.2 M NaCl (not shown).

In *Hbt. salinarum*, DolP is charged with a methylated disulfated tetrasaccharide

An *N*-linked glycan decorating *Hbt. salinarum* glycoproteins was previously reported as being assembled on a DolP carrier (Lechner et al. 1985b). Moreover, this DolP-bound glycan was also deemed to be methylated (Lechner et al. 1985a). Given how the *Hbt. salinarum* S-layer glycoprotein and archaellins were shown here to be modified by a different glycan than described in earlier studies, the DolP population in a total *Hbt. salinarum* lipid extract was revisited using reverse phase LC-ESI MS. Such efforts generated an MS/MS profile that included a peak at *m/z* 856.376, corresponding to the $[M\text{-}2H]^{2-}$ ion of C_{55}-DolP modified by a tetrasaccharide comprising a linking hexose, a sulfated hexuronic acid, a hexuronic acid and a sulfated and methylated hexuronic acid (exact mass, 1712.760 Da) (Figure 3A). Reverse phase LC-ESI MS also produced an MS/MS profile that included a peak at *m/z* 849.370, corresponding to the $[M\text{-}2H]^{2-}$ ion of C_{55}-DolP modified by a tetrasaccharide comprising a linking hexose, a sulfated hexuronic acid, a hexuronic acid and a second sulfated hexuronic acid (exact mass, 1698.744 Da) (Figure 3B). The results also yielded an MS/MS profile that contained a peak at *m/z* 816.392, corresponding to the $[M\text{-}2H]^{2-}$ ion of C_{55}-DolP modified by a tetrasaccharide comprising a linking hexose, two hexuronic acids and a sulfated and methylated hexuronic acid (exact mass, 1633.811 Da) (Figure 3C). An MS/MS profile that presented a peak at *m/z* 809.401, corresponding to the $[M\text{-}2H]^{2-}$ ion of C_{55}-DolP modified by a tetrasaccharide comprising a linking hexose, two hexuronic acids and a sulfated hexuronic acid (exact mass, 1619.795 Da), was also obtained (Figure 3D). Each MS/MS profile also included peaks corresponding to the $[M\text{-}2H]^{2-}$ and $[M\text{-}H]^{-}$ ions of predicted breakdown products. Finally, a minor population of DolP bearing the tetrasaccharide not modified by either sulfate or methyl groups was also observed (not shown).

In agreement with earlier efforts (Lechner et al. 1985a), no methylation of the protein-bound tetrasaccharide decorating the *Hbt. salinarum* S-layer glycoprotein and archaellins was seen (not shown).

Methylated disulfated tetrasaccharide-bearing DolP accumulates in the absence of AglB

In Archaea, the oligosaccharyltransferase AglB is required for addition of the DolP-bound glycan to target Asn residues (Jarrell et al.

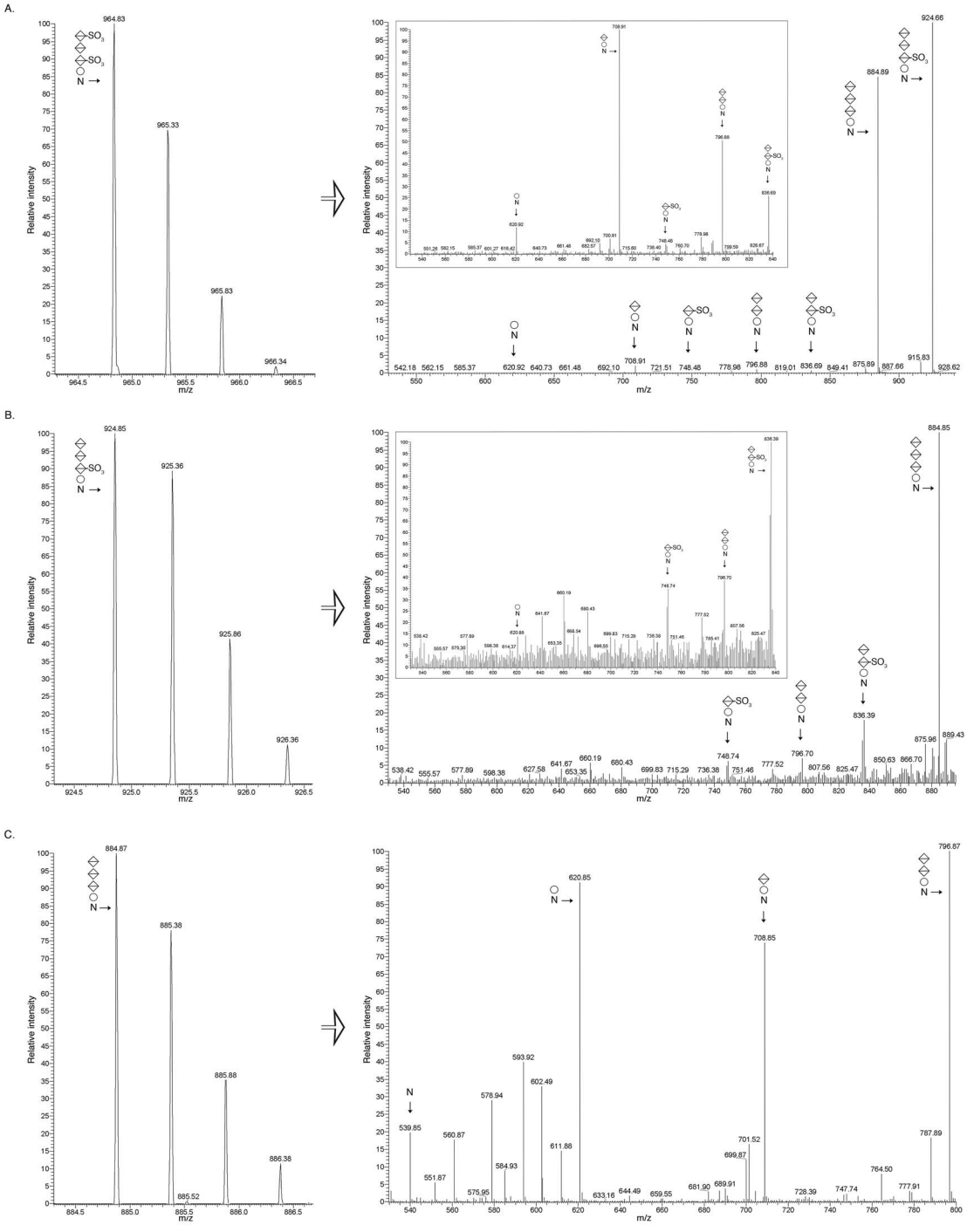

Fig. 2. *Halobacterium salinarum* archaellins are also modified by a disulfated tetrasaccharide. LC-ESI MS (left panels) and MS/MS (right panels) identified a modified asparagine in a peptide common to FlaA2/FlaB1/FlaB3 as being modified by a tetrasaccharide comprising a hexose, a sulfated hexuronic acid, a hexuronic acid and a sulfated hexuronic acid (**A**), the same peptide modified by a tetrasaccharide comprising a hexose, two hexuronic acids and a sulfated hexuronic acid (**B**) and the same peptide modified by a tetrasaccharide comprising a hexose and three hexuronic acids (**C**). In the MS/MS profiles, selected regions are expanded to highlight specific peaks (right panels, insets). The circles correspond to hexoses, the split diamonds correspond to hexuronic acids and the N corresponds to the Asn-56/80/56-containing peptide.

2014). Indeed, in the case of *Hbt. salinarum*, the involvement of AglB in adding an *N*-linked tetrasaccharide to archaellins has been experimentally demonstrated (Zaretsky et al. 2019). Deletion of *aglB* did not, however, prevent the assembly of DolP bearing the disulfated tetrasaccharide, as comparable amounts of a peak at *m/z* 849.37 (corresponding to the $[M\text{-}2H]^{2-}$ ion) of this species were observed in MS/MS profiles of both the parent and deletion strains (Figure 4, upper and lower MS profiles, respectively). However, the amount of

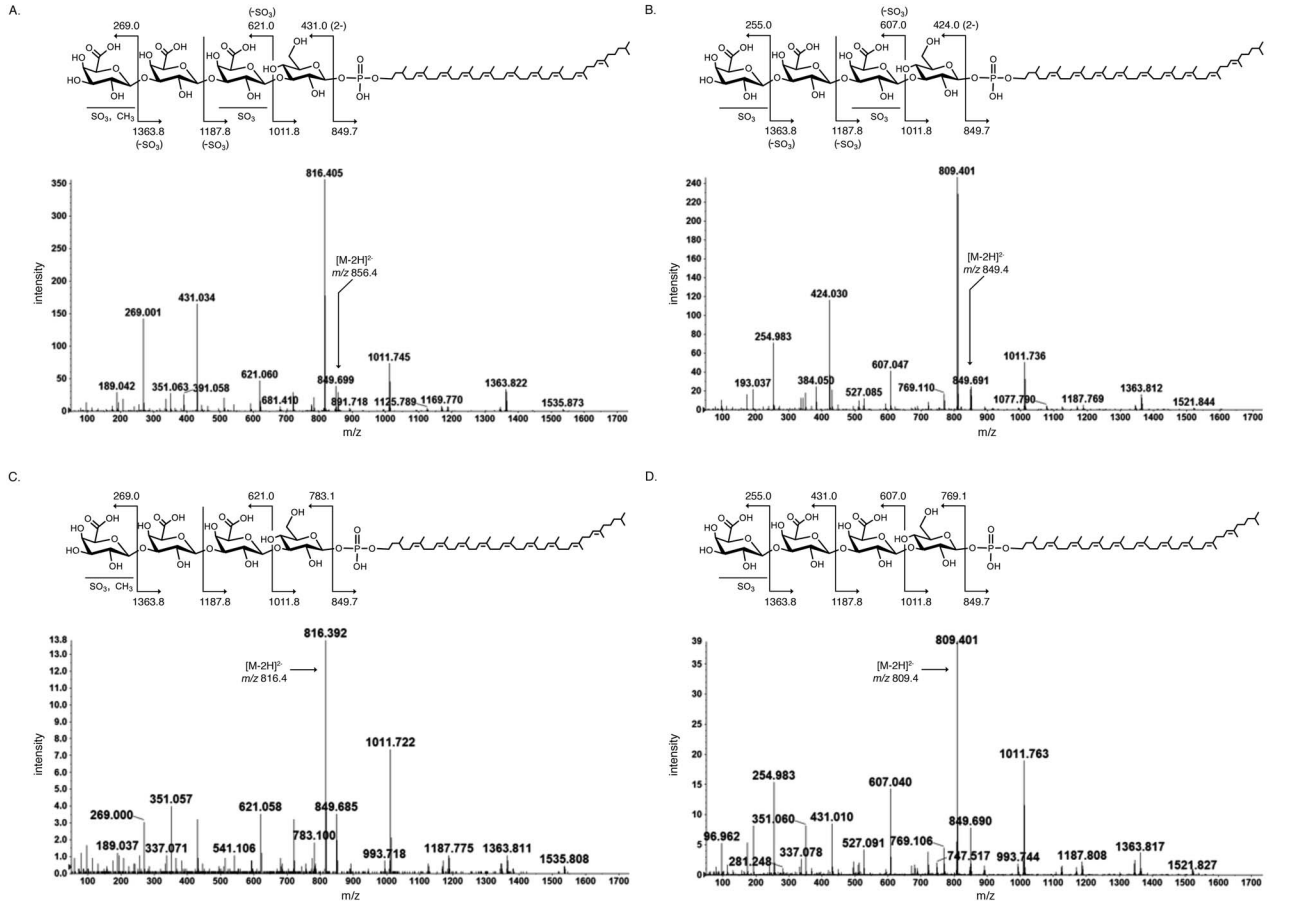

Fig. 3. *Halobacterium salinarum* DolP is modified by a methylated disulfated tetrasaccharide. Reverse-phase LC-ESI MS analysis of the DolP population in a total *Hbt. salinarum* lipid extract contains DolP modified by a tetrasaccharide comprising a hexose, a sulfated hexuronic acid, a hexuronic acid and a methylated sulfated hexuronic acid (**A**), a hexose, a sulfated hexuronic acid, a hexuronic acid and a sulfated hexuronic acid (**B**), a hexose, two hexuronic acids and a methylated sulfated hexuronic acid (**C**) and a hexose, two hexuronic acids and a sulfated hexuronic acid (**D**). In each of the MS/MS profiles, the peak corresponding to the $[M\text{-}2H]^{2-}$ ion of the modified DolP species is indicated. Above each MS/MS profile, the breakdown diagram obtained and the masses of the $[M\text{-}H]^{-}$ ions are shown. Where $[M\text{-}2H]^{2-}$ ions were observed, (2-) appears in the breakdown diagram. Likewise, when the mass observed reflects a fragment lacking the sulfate group ($-SO_3$) appears. Since the precise locations of the sulfate and methyl groups are not clear, their presence is indicated by $-SO_3$ or $-CH_3$ below each modified sugar in the tetrasaccharide detected.

DolP bearing the methylated and disulfated tetrasaccharide, seen in the MS/MS profiles as a peak at *m/z* 856.376 (corresponding to the $[M\text{-}2H]^{2-}$ ion), was considerably higher in the Δ*aglB* cells.

Discussion

In 1976, the *Hbt. salinarum* S-layer glycoprotein provided the first example of N-glycosylation outside the Eukarya (Mescher and Strominger 1976). Over the following decade, considerable progress was made in defining the composition of a glycan *N*-linked to the S-layer glycoprotein and archaellins in this haloarchaeon. Specifically, the glycan was described as a tetrasaccharide comprising Glc and three GlcAs, with each GlcA being sulfated, as a tetrasaccharide comprising Glc-$(GlcA)_2$-Glc or as the pentasaccharide Glc-$(GlcA)_3$-Glc (Wieland et al. 1980, 1983, 1985; Lechner et al. 1985a). Furthermore, at least one GlcA unit was described as being replaced by iduronic acid (Wieland et al. 1986). More recently, the *N*-linked glycan was described as a nonsulfated tetrasaccharide comprising a hexose and three hexuronic acids (Zaretsky et al. 2019). These early efforts also included steps aimed at defining aspects of the biosynthetic pathway involved. Such studies identified DolP as the lipid carrier upon which the glycan is assembled (Lechner et al. 1985b) and predicted the methylation of a Glc found at the nonreducing end of DolP-bound glycan (yet absent from the protein-bound glycan) as being important for transfer of the lipid-linked glycan to the target protein (Lechner et al. 1985a). The use of LC-ESI MS in the present study offered a more precise description of the *N*-linked tetrasaccharide decorating *Hbt. salinarum* glycoproteins and provided insight into the pathway used to assemble this glycan.

The MS and derived MS/MS profiles from two S-layer glycoprotein-derived peptides containing modified asparagine residues and from modified asparagine-containing peptides generated from four of the five *Hbt. salinarum* archaellins are consistent with the presence of an *N*-linked a tetrasaccharide comprising a hexose, a sulfated hexuronic acid, a hexuronic acid and a second sulfated hexuronic acid. The same samples also included the same glycopeptides lacking either the sulfate group on the fourth sugar or both sulfate groups. At the same time, the DolP-bound version of the same tetrasaccharide presented sulfate groups on the second and fourth sugars, on the fourth sugar alone or not at all. Although

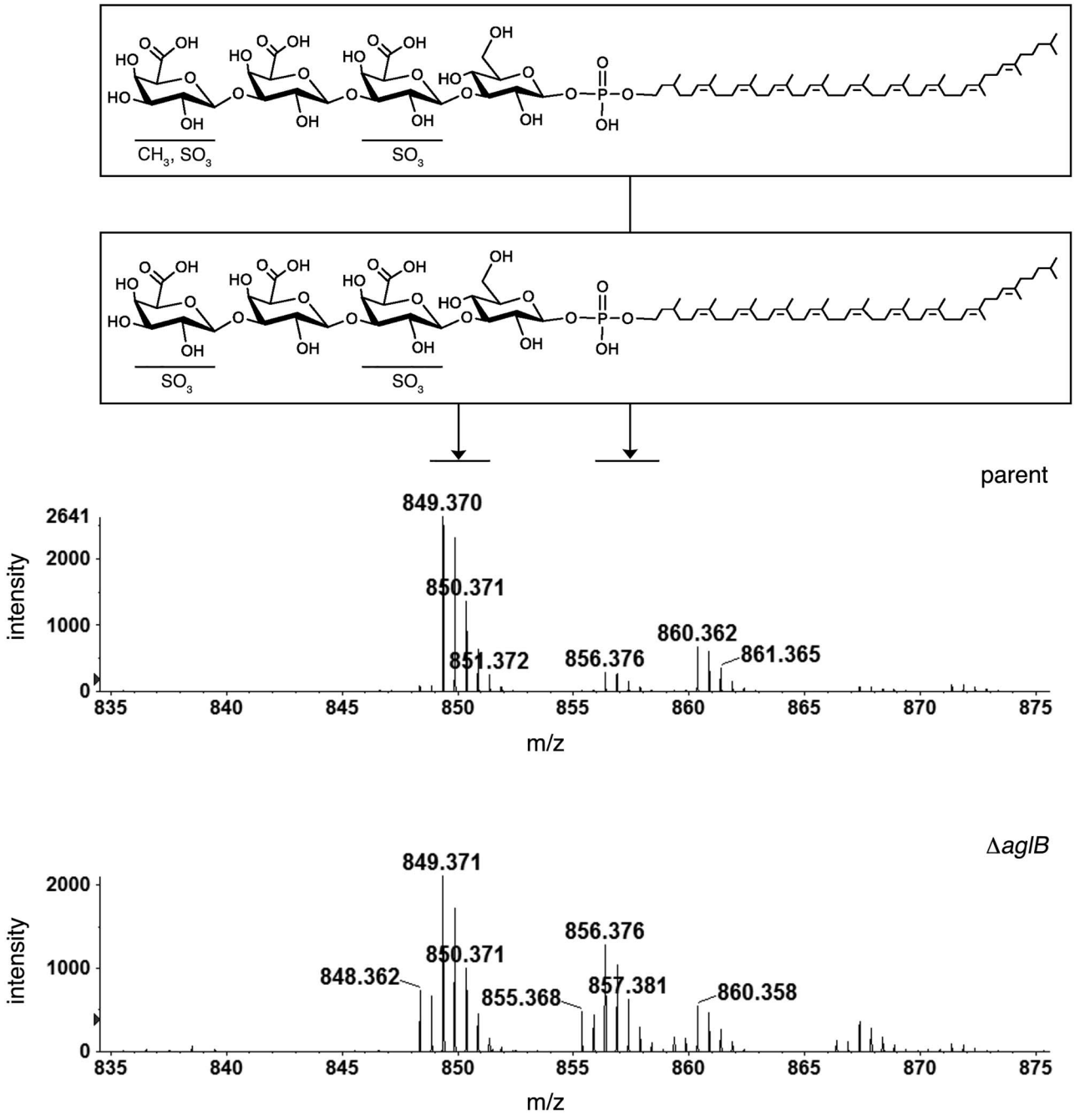

Fig. 4. In the absence of AglB, DolP modified by the methylated disulfated tetrasaccharide accumulates. The DolP populations of total lipid extracts from *Hbt. salinarum* parent (top profile) and Δ*aglB* (bottom profile) strains were assessed by reverse-phase LC-ESI MS in the negative ion mode. The positions of $[M\text{-}H]^-$ ions corresponding to DolP modified by a tetrasaccharide comprising a hexose, a sulfated hexuronic acid, a hexuronic acid and a methylated sulfated hexuronic acid (schematically depicted in the top diagram) and by a tetrasaccharide comprising a hexose, a sulfated hexuronic acid, a hexuronic acid and a sulfated hexuronic acid (schematically depicted in the bottom diagram) are indicated.

the precise carbon modified by the sulfate group was not identified in any of these instances, these results, nonetheless, confirm the earlier claim of glycan sulfation occurring at the lipid-linked stage (Lechner et al. 1985b). At present, it is not clear whether the observed differences in sulfation at both the lipid- and protein-linked levels reflect natural heterogeneity and/or the loss of highly labile sulfate groups during sample preparation and/or analysis. A similar situation was presented by studies of N-glycosylation in the hyperthermophilic archaea *Archaeoglobus fulgidus*, where not all of the linking Glc was sulfated (Fujinami et al. 2015). Liability of sugar-bound sulfate groups could explain our failure to detect sulfation of the protein-bound tetrasaccharide in an earlier study of the *N*-linked tetrasaccharide *Hbt. salinarum* decorating archaellins; here, the archaellins were recovered from the culture medium after several centrifugation and resuspension steps (Zaretsky et al. 2019). Such loss of sulfate groups could also explain why in that version of the tetrasaccharide presenting a single sulfate group, the hexuronic acid at position 4 was sulfated in the lipid-linked glycan while the

hexuronic acid at position 2 was modified in the protein-bound form. This makes it difficult to draw any conclusions regarding the order of hexuronic acid sulfation. At the same time, the fact that no sulfation of the third tetrasaccharide sugar was detected at either the lipid- or protein-linked stages argues for specificity in the sulfation process. Still, little is known of the sulfation process itself, although in the thermoacidophilic archaea *Sulfolobus acidocaldarius*, Agl3 was shown to be a UDP-sulfoquinovose synthase and important for N-glycosylation, suggesting that at least in this species, sulfation occurs at the nucleotide-linked sugar level (Meyer et al. 2011).

In addition to outstanding questions regarding the sulfation process, the purpose of such glycan sulfation is also not clear at this time. It had been proposed that sulfation of the *N*-linked glycan is an adaptation of *Hbt. salinarum* to life in hypersaline conditions, given how *Hfx. volcanii*, a haloarchaeon that grows optimally at lower salt concentrations than does *Hbt. salinarum*, decorates its glycoproteins with a glycan that is not sulfated (Mengele and Sumper 1992). It was proposed that sulfation of glycans decorating *Hbt. salinarum* glycoproteins increases the number of negative charges on the cell surface so as to help the cells remain soluble in their hypersaline surroundings. However, it was subsequently reported that *Hfx. volcanii* modifies its N-glycosylation profile when grown in low salt by generating a sulfated tetrasaccharide; this sulfated tetrasaccharide is not assembled when the cells are raised at higher salinity (Kaminski, Guan, et al. 2013a). In addition, the present study failed to observe any differences in *Hbt. salinarum N*-linked tetrasaccharide sulfation when the cells were grown in low, medium or high salt levels.

The present study also confirmed the earlier finding of methylation of the glycan at the lipid-linked stage but not when bound to protein, although such modification was detected on the final hexuronic acid here, rather than on a Glc at the nonreducing end, as reported previously (Lechner et al. 1985a). In the present study, the precise position of the methyl group was not determined. The observation that the methylated version of the tetrasaccharide accumulated in cells lacking the oligosaccharyltransferase AglB could argue how such methylation is important for transfer of the lipid-linked glycan to select asparagine residues of a target protein, rather than for delivery of the lipid-linked glycan across the membrane, as previously proposed (Lechner et al. 1985a), given how AglB acts on the external surface of the cell, after translocation of the lipid-linked glycan across the membrane. While nothing is presently known of the enzyme responsible for delivering DolP-linked glycans across the archaeal plasma membrane, the central role of AglB in the N-glycosylation pathways of *Hbt. salinarum* and other Archaea has been directly shown (Jarrell et al. 2014; Zaretsky et al. 2019). To the best of our knowledge, transient methylation of the lipid-linked glycan and its importance for later steps in the N-glycosylation process have not been reported for any organism other than *Hbt. salinarum*. It is possible that such methylation is related to the use of DolP as the glycan lipid carrier by *Hbt. salinarum*, rather than dolichol pyrophosphate, as is the case in Eukarya and other Archaea (Guan et al. 2016; Taguchi et al. 2016). This, however, is unlikely, since no need for transient methylation has been reported for other archaeal N-glycosylation pathways in which DolP serves as glycan lipid carrier, including those of *Hfx. volcanii*, *Haloarcula marismortui*, *Methanococcus maripaludis* and *Methanococcus voltae* (Jarrell et al. 2014). Moreover, it is unclear why the actions of *Hbt. salinarum* AglB would involve transient methylation of the DolP-linked glycan, since the *Hbt. salinarum* enzyme is able to functionally replace its counterpart in *Hfx. volcanii*, where no such methylation occurs (Cohen-Rosenzweig et al. 2014). Indeed, none of the AglB proteins characterized to date has displayed a requirement for such methylation (Kohda 2018). It is conceivable that transient glycan methylation is associated with more efficient AglB-mediated transfer of the glycan from the lipid carrier to the protein target. Until the methyltransferase responsible for such transient methylation has been identified and thus the effect of its deletion can be assessed, the reason for transient methylation of the DolP-linked disulfated tetrasaccharide in *Hbt. salinarum* N-glycosylation remains unclear.

To date, the only component of the *Hbt. salinarum* N-glycosylation pathway to be identified and functionally characterized is AglB (Zaretsky et al. 2019). The observation that many members of the Euryarchaeota (a subdivision of the domain Archaea) cluster genes encoding N-glycosylation pathway components into an island or cluster anchored by *aglB* led to the identification of other putative participants in the *Hbt. salinarum* N-glycosylation pathway (Magidovich and Eichler 2009; Kaminski, Lurie-Weinberger, et al. 2013b; Kandiba and Eichler 2015; Nikolayev et al. 2020). These include several predicted glycosyltransferases, a possible isomerase and a putative methyltransferase (Kandiba and Eichler 2015). Indeed, several of these proteins could functionally replace known components of the *Hfx. volcanii* N-glycosylation process (Cohen-Rosenzweig et al. 2014; Kandiba and Eichler 2015). With the availability of gene deletion techniques for *Hbt. salinarum* (Peck et al. 2000), together with the MS protocols described here, efforts can now focus on identifying those enzymes that participate in the biosynthesis of the *N*-linked tetrasaccharide first assembled on DolP and then bound to glycoproteins in this organism.

Materials and methods

Cell growth

Halobacterium salinarum parent and Δ*aglB* strains (Zaretsky et al. 2019) were grown in medium containing (per L) 250 g NaCl, 20 g $MgSO_4{\cdot}7H_2O$, 3 g sodium citrate, 2 g KCl and 10 g peptone and supplemented with 50 μg/mL uracil at 42°C.

Isolation of the *Hbt. salinarum* lipid fraction

To extract the total lipid content of *Hbt. salinarum*, the protocol described by Kelleher et al. (2001) was employed, with minor modifications. *Hbt. salinarum* cells were harvested (8,000*g*, 30 min, 4°C); the pellet was resuspended in 2 M NaCl, 50 mM Tris–HCl, pH 7.2, centrifuged again (8,000*g*, 90 min, 4°C) and the pellet was frozen at −20°C until extraction was performed. At that point, the pelleted cells (~15 g) were thawed, resuspended in 20 mL double-distilled water (DDW) and DNase (1.7 μg/mL; Sigma, St. Louis, MO) and stirred overnight at room temperature, followed by sonication on ice at room temperature (2 s on, 5 s off, for a total of 1 min; Vibracell VCX750 ultrasonic cell disrupter, Sonics, Newtown, CT). After sonication, the cell suspension was centrifuged for 30 min at 11,000 rpm in a SW-40 rotor at 4°C to clear non-broken cells and other debris. The supernatant was transferred into fresh tubes and centrifuged for an additional 45 min at 36,000 rpm in a SW-40 rotor at 4°C. The resulting supernatant was removed and the pellet was resuspended in 35 mL homogenization buffer (150 mM NaCl, 50 mM Tris–HCl, pH 8) containing 50 mL $CHCl_3$:CH_3OH (3:2; v/v) at 4°C and homogenized using a Pyrex Potter-Elvehjem tissue grinder (Thomas Scientific). After homogenization, 65 mL cold (4°C) $CHCl_3$:CH_3OH (3:2; v/v) were added and the homogenate was mixed by vigorous shaking before centrifugation (3,400*g*, 15 min, 4°C). The resulting

clear upper aqueous and lowest organic phases were removed and the middle (solid) phase was resuspended in 75 mL of $CHCl_3$:CH_3OH (3:2; v/v) containing 1 mM $MgCl_2$ at room temperature. After vigorous rehomogenization, the suspension was adjusted to a total volume of 150 mL and centrifuged for 15 min (3,400*g*, 4°C). The supernatant was removed and the pellet was suspended in 150 mL CH_3OH containing 4 mM $MgCl_2$ before centrifugation (3,400*g*, 15 min, 4°C). These steps were repeated and the resulting pellet was suspended in 150 mL $CHCl_3$:CH_3OH:DDW (10:10:3; v/v/v) and centrifuged in a swing-out rotor (1,000 rpm) for 15 min at 22°C. The supernatant was removed and stored while the pellet was re-extracted with 100 mL $CHCl_3$:CH_3OH:DDW (10:10:3; v/v/v) at 37°C and centrifuged as above. The supernatants obtained from the first and second extractions were combined, filtered through glass wool and the ensuing solution was evaporated at 30°C. Thereafter, any remaining solvents were removed using a stream of nitrogen. The dried extracts were then subjected to analysis by liquid chromatography coupled with mass spectrometry, as described below.

Isolation of *Hbt. salinarum* archaellins

The five *Hbt. salinarum* archaellins (FlaA1, FlaA2, FlaB1, FlaB2 and FlaB3) were enriched from spent growth medium as previously described (Alam and Oesterhelt 1984). Briefly, cultures were grown to stationary (OD_{600} ~2.0) phase and held at room temperature without shaking for 24 h. The cultures were centrifuged for 30 min (6,000*g*, 15°C). The supernatant was collected and centrifuged again for 15 min (16,000*g*, 15°C). The supernatant was centrifuged again for 2 h (40,000*g*, 4°C). The pellet was resuspended by shaking in 1 mL of 4 M basal salt solution (250 g NaCl, 20 g $MgSO_4 \cdot 7H_2O$, 3 g sodium citrate, 2 g KCl per L) and heated for 10 min at 90°C. The heated suspension was centrifuged for 15 min (16,000*g*, 15°C). The resulting supernatant was maintained at 4°C for 24 h and centrifuged for 2 h (40,000*g*, 4°C). After removal of the supernatant, the pellet was resuspended in sample buffer and separated by 12% SDS-PAGE and stained with Coomassie InstantBlue (Expedeon).

LC-ESI MS

Reverse-phase LC-ESI-MS of the *Hbt. salinarum* lipid extract was performed using a Shimadzu LC system (comprising a solvent degasser, two LC-10A pumps and a SCL-10A system controller) coupled to a TripleTOF5600 mass spectrometer (Sciex, Framingham, MA). LC was operated at a flow rate of 200 μL/min with a linear gradient as follows: 100% of mobile phase A was held isocratically for 2 min and then linearly increased to 100% mobile phase B over 14 min and held at 100% B for 4 min. Mobile phase A consisted of methanol/acetonitrile/aqueous 1 mM ammonium acetate (60/20/20, v/v/v). Mobile phase B consisted of 100% ethanol containing 1 mM ammonium acetate. A Zorbax SB-C8 reversed-phase column (5 μm, 2.1 × 50 mm) was obtained from Agilent (Palo Alto, CA). The negative ion mode MS operating conditions are as follows: IS = −4500 V, CUR = 20 psi, GS1 = 20 psi, DP = −55 V, and FP = −150 V. For MS/MS, collision-induced dissociation was performed with collision energy ranging from 40 to 70 V (laboratory frame of energy) and with nitrogen as the collision gas. Data acquisition and analysis were performed using the instrument's Analyst QS software.

For LC-ESI MS analysis, the *Hbt. salinarum* S-layer glycoprotein, recognized via its unique SDS-PAGE migration pattern, was subjected to in-gel digestion, as were the isolated archaellins. S-layer glycoprotein- and archaellin-containing bands were excised from SDS-PAGE gels using a clean scalpel, destained in 400 μL of 50% (vol/vol) acetonitrile (Sigma) in 40 mM NH_4HCO_3, pH 8.4, dehydrated with 100% acetonitrile and dried using a SpeedVac drying apparatus. The proteins in the gel slices were reduced with 10 mM dithiothreitol (Sigma) in 40 mM NH_4HCO_3 at 56°C for 60 min and then alkylated for 45 min at room temperature with 55 mM iodoacetamide in 40 mM NH_4HCO_3. The gel pieces were washed with 40 mM NH_4HCO_3 for 15 min, dehydrated with 100% acetonitrile and SpeedVac-dried. The gel slices were rehydrated with 12.5 ng/μL of mass spectrometry (MS)-grade Trypsin Gold (Promega) in 40 mM NH_4HCO_3 and incubated overnight at 37°C. The protease-generated peptides were extracted with 0.1% (v/v) formic acid in 20 mM NH_4HCO_3, followed by sonication for 20 min at room temperature, dehydration with 50% (v/v) acetonitrile and additional sonication. After three rounds of extraction, the gel pieces were dehydrated with 100% acetonitrile and dried completely with a SpeedVac. In some cases, 12.5 ng/μL Glu-C (V8) protease (Promega, sequencing-grade) in 40 mM NH_4HCO_3 were added. After an overnight incubation at 37°C, these samples were dried completely with a SpeedVac. Both trypsin- and trypsin and Glu-C-treated samples were resuspended in 5% (v/v) acetonitrile containing 1% formic acid (v/v) and infused into the mass spectrometer using static nanospray Econotips (New Objective, Woburn, MA). The protein digests were separated on-line by nano-flow reverse-phase liquid chromatography by loading onto a 150 mm by 75 μm (internal diameter) by 365 μm (external diameter) Jupifer pre-packed fused silica 5 μm C_{18} 300 Å reverse-phase column (Thermo Fisher Scientific, Bremen, Germany). The sample was eluted into the LTQ Orbitrap XL mass spectrometer (Thermo Fisher Scientific) using a 60-min linear gradient of 0.1% formic acid (v/v) in acetonitrile/0.1% formic acid (1:19, by volume) to 0.1% formic acid in acetonitrile/0.1% formic acid (4:1, by volume) at a flow rate of 300 nL/min.

Supplementary data

Supplementary data are available at *Glycobiology* online.

Data Availability

All data are contained in the manuscript.

Acknowledgements

The authors thank Dr. Gabriela Ring for contributions made in the early stages of this project.

Funding

This work supported by the National Institutes of Health [grant R01AI148366 to Z.G.] and the Israel Science Foundation [grant 414/20 to J.E.].

Abbreviations

DolP, dolichol phosphate; Glc, glucose; GlcA, glucuronic acid; Hex, hexose; HexA, hexuronic acid; LC-ESI MS, liquid chromatography-electrospray ionization mass spectrometry.

References

Aebi M. 2013. N-linked protein glycosylation in the ER. *Biochim Biophys Acta*. 1833:2430–2437.

Alam M, Oesterhelt D. 1984. Morphology, function and isolation of halobacterial flagella. *J Mol Biol*. 176:459–475.

Burda P, Aebi M. 1999. The dolichol pathway of N-linked glycosylation. *Biochim Biophys Acta*. 1426:239–257.

Cohen-Rosenzweig C, Guan Z, Shaanan B, Eichler J. 2014. Substrate promiscuity: AglB, the archaeal oligosaccharyltransferase, can process a variety of lipid-linked glycans. *Appl Environ Microbiol*. 80:486–496.

Eichler J. 2013. Extreme sweetness: Protein glycosylation in Archaea. *Nat Rev Microbiol*. 11:151–156.

Eichler J, Guan Z. 2017. Lipid sugars carriers at the extremes: The phosphodolichols Archaea use in N-glycosylation. *Biochim Biophys Acta*. 1862:589–599.

Fujinami D, Nyirenda J, Matsumoto S, Kohda D. 2015. Structural elucidation of an asparagine-linked oligosaccharide from the hyperthermophilic archaeon, *Archaeoglobus fulgidus*. *Carbohydr Res*. 413: 55–62.

Guan Z, Delago A, Nussbaum P, Meyer B, Albers SV, Eichler J. 2016. N-glycosylation in the thermoacidophilic archaeon *Sulfolobus acidocaldarius* involves a short dolichol pyrophosphate carrier. *FEBS Lett*. 590:3168–3178.

Hartley MD, Imperiali B. 2012. At the membrane frontier: A prospectus on the remarkable evolutionary conservation of polyprenols and polyprenylphosphates. *Arch Biochem Biophys*. 517:83–97.

Jarrell KF, Albers SV. 2012. The archaellum: An old motility structure with a new name. *Trends Microbiol*. 20:307–312.

Jarrell KF, Ding Y, Meyer BH, Albers SV, Kaminski L, Eichler J. 2014. N-linked glycosylation in Archaea: A structural, functional, and genetic analysis. *Microbiol Mol Biol Rev*. 78:304–341.

Jones MB, Rosenberg JN, Betenbaugh MJ. Krag SS. 2009. *Structure and synthesis of polyisoprenoids used in N-glycosylation across the three domains of life*. *Biochim Biophys Acta* 1790:485–494.

Kaminski L, Guan Z, Yurist-Doutsch S, Eichler J. 2013a. Two distinct N-glycosylation pathways process the *Haloferax volcanii* S-layer glycoprotein upon changes in environmental salinity. *MBio*. 4:e00716–e00713.

Kaminski L, Lurie-Weinberger MN, Allers T, Gophna U, Eichler J. 2013b. Phylogenetic- and genome-derived insight into the evolution of N-glycosylation in Archaea. *Mol Phylogenet Evol*. 68: 327–339.

Kandiba L, Eichler J. 2015. Deciphering a pathway of *Halobacterium salinarum* N-glycosylation. *MicrobiologyOpen*. 4:28–40.

Kohda D. 2018. Structural basis of protein Asn-glycosylation by oligosaccharyltransferases. *Adv Exp Med Biol*. 1104:171–199.

Kelleher DJ, Karaoglu D, Gilmore R. 2001. Large-scale isolation of dolichol-linked oligosaccharides with homogeneous oligosaccharide structures: Determination of steady-state dolichol-linked oligosaccharide compositions. *Glycobiology*. 11:321–333.

Lechner J, Wieland F, Sumper M. 1985a. Transient methylation of dolichyl oligosaccharides is an obligatory step in halobacterial sulfated glycoprotein biosynthesis. *J Biol Chem*. 260:8984–8989.

Lechner J, Wieland F, Sumper M. 1985b. Biosynthesis of sulfated saccharides N-glycosidically linked to the protein via glucose. Purification and identification of sulfated dolichyl monophosphoryl tetrasaccharides from halobacteria. *J Biol Chem*. 260:860–866.

Lechner J, Sumper M. 1987. The primary structure of a procaryotic glycoprotein. Cloning and sequencing of the cell surface glycoprotein gene of halobacteria. *J Biol Chem*. 262:9724–9729.

Lechner J, Wieland F. 1989. Structure and biosynthesis of prokaryotic glycoproteins. *Annu Rev Biochem*. 58:173–194.

Magidovich H, Eichler J. 2009. Glycosyltransferases and oligosaccharyltransferases in Archaea: Putative components of the *N*-glycosylation pathway in the third domain of life. *FEMS Microbiol Lett*. 300:122–130.

Mengele R, Sumper M. 1992. Drastic differences in glycosylation of related S-layer glycoproteins from moderate and extreme halophiles. *J Biol Chem*. 267:8182–8185.

Mescher MF, Strominger JL. 1976. Purification and characterization of a prokaryotic glycoprotein from the cell envelope of *Halobacterium salinarium*. *J Biol Chem*. 251:2005–2014.

Meyer BH, Zolghadr B, Peyfoon E, Pabst M, Panico M, Morris HR, Haslam SM, Messner P, Schäffer C, Dell A, et al. 2011. Sulfoquinovose synthase - an important enzyme in the N-glycosylation pathway of *Sulfolobus acidocaldarius*. *Mol Microbiol*. 82:1150–1163.

Nikolayev S, Cohen-Rosenzweig C, Eichler J. 2020. Evolutionary considerations of the oligosaccharyltransferase AglB and other aspects of N-glycosylation across Archaea. *Mol Phylogenet Evol*. 153:106951.

Ng WV, Kennedy SP, Mahairas GG, Berquist B, Pan M, Shukla HD, Lasky SR, Baliga NS, Thorsson V, Sbrogna J, et al. 2000. Genome sequence of *Halobacterium* species NRC-1. *Proc Natl Acad Sci U S A*. 97:12176–12181.

Nothaft H, Szymanski CM. 2013. Bacterial protein N-glycosylation: New perspectives and applications. *J Biol Chem*. 288:6912–6920.

Peck RF, DasSarma S, Krebs MP. 2000. Homologous gene knockout in the archaeon *Halobacterium salinarum* with *ura3* as a counterselectable marker. *Mol Microbiol*. 35:667–676.

Schwarz F, Aebi M. 2011. Mechanisms and principles of N-linked protein glycosylation. *Curr Opin Struct Biol*. 21:576–582.

Swiezewska E, Danikiewicz W. 2005. Polyisoprenoids: Structure, biosynthesis and function. *Prog Lipid Res*. 44:235–258.

Taguchi Y, Fujinami D, Kohda D. 2016. Comparative analysis of archaeal lipid-linked oligosaccharides that serve as oligosaccharide donors for Asn glycosylation. *J Biol Chem*. 291:11042–11054.

Trachtenberg S, Pinnick B, Kessel M. 2000. The cell surface glycoprotein layer of the extreme halophile *Halobacterium salinarum* and its relation to *Haloferax volcanii*: Cryo-electron tomography of freeze-substituted cells and projection studies of negatively stained envelopes. *J Struct Biol*. 130:10–26.

Wieland F. 1988. Structure and biosynthesis of prokaryotic glycoproteins. *Biochimie*. 70:1493–1504.

Wieland F, Dompert W, Bernhardt G, Sumper M. 1980. Halobacterial glycoprotein saccharides contain covalently linked sulphate. *FEBS Lett*. 120:110–114.

Wieland F, Heitzer R, Schaefer W. 1983. Asparaginylglucose: Novel type of carbohydrate linkage. *Proc Natl Acad Sci U S A*. 80:5470–5474.

Wieland F, Paul G, Sumper M. 1985. Halobacterial flagellins are sulfated glycoproteins. *J Biol Chem*. 260:15180–15185.

Wieland F, Lechner J, Sumper M. 1986. Iduronic acid: Constituent of sulphated dolichyl phosphate oligosaccharides in halobacteria. *FEBS Lett*. 195:77–81.

Zaretsky M, Darnell CL, Schmid AK, Eichler J. 2019. *N*-Glycosylation is important for *Halobacterium salinarum* archaellin expression, archaellum assembly and cell motility. *Front Microbiol*. 10:1367.